BETTII: A pathfinder for high angular resolution observations of star-forming regions in the far-infrared

by

Maxime J. Rizzo

Dissertation submitted to the Faculty of the Graduate School of the
University of Maryland, College Park in partial fulfillment
of the requirements for the degree of
Doctor of Philosophy
2016

Advisory Committee:
Professor Lee G. Mundy, Chair/Advisor (UMD)
Dr. Stephen A. Rinehart, Co-Advisor (NASA GSFC)
Professor Andrew Harris (UMD)
Dr. Mark Wolfire (UMD)
Dr. Alison Nordt (Lockheed Martin)
Professor Eun-Suk Seo, Dean's representative (UMD)

To Michelle, my parents, and my brother.

Acknowledgements

The acknowledgments and the people to thank go here, don't forget to include your project advisor...

Contents

Acknowledgements **iii**

Contents **v**

List of Tables **ix**

List of Figures **xi**

I Star formation in clustered environments **5**
I.1 Molecular Clouds 5
I.2 Star formation 7
I.2.1 Standard models 7
I.2.1.1 Gravitational collapse 7
I.2.1.2 YSO classification and characteristics 11
I.2.2 Mass accretion in clusters 15
I.3 Dust as a tracer of star formation 17
I.3.1 Dust populations and properties 18
I.3.2 Basics of dust extinction 19
I.3.3 Radiative transfer modeling 21
I.3.4 Observing star formation 23

List of Tables

List of Figures

I.1 Protostar 10
I.2 Early evolution of YSOs 12
I.3 Late evolution of YSOs 13
I.4 Scenarios of clustered star formation 17

Introduction

In order to improve the mind, we ought less to learn, than to contemplate.

R. Descartes

The work presented in this thesis is centered around the design, development, and testing of an astronomical balloon-borne telescope called BETTII: the Balloon Experimental Twin Telescope for Infrared Interferometry. Developed at NASA Goddard Space Flight Center, this instrument is exploring a relatively new observation technique called "Double-Fourier" interferometry, which could lead to future space-borne telescopes with high angular resolution in the far-infrared regime. Various fields in astronomy would benefit from such enhanced capability, as demonstrated by the success of far-infrared single-aperture telescopes such as WISE, *Spitzer* and *Herschel*.

More than just a pathfinder, BETTII is a scientific instrument in its own right. For its first flights, it will study regions of clustered star formation in unprecedented details, providing almost an order of magnitude better spatial resolution than any existing or past far-IR facility.

This work describes some aspects of my involvement with BETTII as well as my contributions to the scientific field of clustered star formation using another far-IR facility, the Stratospheric Observatory for Infrared Astronomy (SOFIA). The thesis is organized as follows:

- Chapter I describes the framework and current understanding of how stars are forming in clusters, and lays out the key tools that we use to study these regions.

- Chapter **??** is a study of nearby star-forming clusters using new data that we obtained with the SOFIA observatory. SOFIA offers moderately high angular resolution, which we use to improve the study of the brightest, densest regions of star formation. This work is to be submitted for publication shortly after the conclusion of this dissertation.

- Chapter **??** describes the physical principles of interferometry which drive the design of the balloon instrument. We predict the sensitivity of the BETTII instrument and identify scientific targets and calibrators that are suitable for our first flights.

- Chapter **??** is a standalone, refereed paper that was published in 2015 on the spectral sensitivity of double-Fourier interferometers in general. It proposes a mathematical framework to analyze the sensitivity of such instruments to various types of noise sources. We apply those findings to the case of BETTII.

- Chapter **??** discusses the design of the control system for BETTII, which presents unique challenges compared to any other balloon-borne instrument. We also discuss the controls algorithm that is used in flight to properly estimate the orientation of the payload, a key requirement to achieve successful interferometry.

- Chapter **??** shows results of the implementation of the control system on BETTII. This consists of laboratory and on-sky testing of BETTII at GSFC.

- Chapter **??** summarizes our findings and discusses the path forward for the BETTII project.

BETTII will be shipping out to Fort Sumner, New Mexico, for its first balloon flight in early August. The flight window is from mid to late September. The technical work in chapters III to VI plays a key role in the success of this first flight.

Chapter I

Star formation in clustered environments

This chapter is an introduction to some of the concepts which play a role in the formation of stars. First, we discuss properties of the molecular clouds which are the sites of star formation. Second, we elaborate on the physics of the star-forming processes and their various stages. Third, we discuss the properties of the dust, which is the main observable which is relevant for the rest of this thesis. This chapter is not meant to be an exhaustive review of the field, but instead introduces the relevant scales, contexts, and metrics associated with the star formation phenomenon, which are important to understand when designing an observatory to study it.

I.1 Molecular Clouds

Molecular clouds are the dense regions of the interstellar medium (ISM) where stars are forming. They contain about half the mass of the ISM in $< 2\%$ of its volume (see Kennicutt et al., 2012, and references therein). High densities ($n \gtrsim 1000\,\mathrm{cm}^{-3}$) of mostly molecular hydrogen and low temperatures ($< 20\,\mathrm{K}$) distinguish molecular clouds from the other major

components of the ISM in galaxies: the Hot Ionized Medium, the Warm Neutral Medium, the Warm Ionized Medium, and the other cold phase of the ISM, the Cold Neutral Medium, which is thought to be the parent region in which molecular clouds are formed. In addition to molecular hydrogen, molecular clouds also contain Helium (cosmic abundance of 10% by number), dust ($\sim 1\%$ by mass), CO ($\sim 1 \times 10^{-4}$ by number), and traces of many other molecules.

Observations reveal that molecular clouds are highly structured with often a filamentary structure on a range of spatial scales (**Heyer:2015ee**; **Andre:2010ka**; **Andre:2014et**; Williams et al., 2000). We are particularly interested in the star formation process in these regions so our focus is on the youngest systems, $\lesssim 2\,\mathrm{Myr}$, where stars are often still embedded and may not have accreted the majority of their final mass.

Approximately 60% of all stars are thought to form in embedded, young stellar clusters with 100 or more stars (Porras et al., 2003; Allen et al., 2007). These >100 star clusters have characteristic sizes of 2-4 parsecs (pc) with peak surface densities of >10 stars per square parsec and a typical median distance between nearest neighbor young stellar objects (YSOs) <0.06 pc (Gutermuth et al., 2009).

Because star-forming clusters are surrounded by interstellar matter from the parent molecular cloud, they usually cannot be studied at optical wavelengths, due to the large obscuration from dust grains along the line of sight. Infrared observations can be used to probe these structures since the dust can acquire sufficient temperature to emit thermally from the mid-infrared through millimeter wavelengths.

The high density of YSOs within clusters, combined with their typical separations of few hundredths of parsecs requires a high angular resolution in order to capture the relevant spatial scales to identify individual sources and probe their physical characteristics.

I.2 Star formation

I.2.1 Standard models

A considerable amount of literature exists on star formation and the various physical processes involved in forming stars (**Evans:1999gz**; **PortegiesZwart:2010kc**; **Hennebelle:2012dk**; e.g. McKee et al., 2007; Kennicutt et al., 2012, and references therein). In this section, we review some of the most standard views that describe how stars are born and grow to acquire their final masses.

I.2.1.1 Gravitational collapse

The simplest way to derive characteristic quantities related to the formation of stars is to consider a pre-stellar core as a spherical clump of uniform, isothermal gas in hydrostatic equilibrium. For such a system, the Virial theorem applies, which describes the balance between the gravitational potential and the kinetic thermal energy within the gas. In other words, in hydrostatic equilibrium, the core's self-gravity is compensated by the internal pressure caused by the temperature of the gas. If the temperature then decreases, or if the core mass increases, the core will contract and become unstable. While simplistic, this treatment leads to a handy derivation of critical timescales, sizes, and masses that form a good starting point for more elaborate theories.

First, it is important to determine what are the characteristic timescales of star formation. In the core with a uniform density, the simplest timescale to define is called the free-fall time t_{ff}: this is the time it takes for the total gravitational collapse of a spherically-symmetric clump of uniform density ρ if only the force of gravity is considered:

$$\mathrm{t_{ff}} \sim \left(\frac{3\pi}{32G\rho}\right)^{1/2} \sim 1\times10^{6}\,\mathrm{yr}\left(\frac{n}{1000\,\mathrm{cm^{-3}}}\right)^{-1/2} = 1\times10^{6}\,\mathrm{yr}\left(\frac{\rho}{4\times10^{-21}\,\mathrm{g\,cm^{-3}}}\right)^{-1/2}, \tag{I.1}$$

where we have substituted a typical value for the particle density in clusters $n \equiv n_{H_2} \approx 1000\,\mathrm{cm^{-3}}$, and converted it as well into a mass density, using a mean molecular weight $\mu = 2.33$ (corresponding to a Helium abundance of 10% in number as in McKee et al. (2007)). The free-fall time is usually a lower limit on the collapse timescale, since there can always be some physical mechanisms such as thermal and turbulent pressure or magnetic fields that will resist gravity and slow down the infall of gas into the potential well.

The other relevant quantity that involves time is the sound speed in the cloud, $c_\mathrm{s} = (kT/(\mu m_H))^{1/2}$, where $\mu \approx 2.33$ is the mean molecular weight of the gas and m_H the mass of hydrogen. For a given spatial scale R, the sound-crossing time is defined as $\mathrm{t_s} = R/c_\mathrm{s} = 4.9\times10^{5}\,\mathrm{yr}\left(\frac{R}{0.1\,\mathrm{pc}}\right)\left(\frac{c_\mathrm{s}}{0.2\,\mathrm{km\,s^{-1}}}\right)^{-1}$. This is the time it takes for a wave to cross the scale R while traveling at the sound speed. Intuitively, if the core has a size R such that $\mathrm{t_{ff}} < \mathrm{t_s}$, it tends to collapse faster than the gas in the cloud can react. This corresponds to a characteristic sizescale that is called the Jeans' length, and corresponds to the characteristic sizescale of gravitational instability within a cloud (McKee et al., 2007):

$$\lambda_\mathrm{J} = c_\mathrm{s}\times\mathrm{t_{ff}} = 0.2\,\mathrm{pc}\left(\frac{c_\mathrm{s}}{0.2\,\mathrm{km\,s^{-1}}}\right)\left(\frac{n}{1000\,\mathrm{cm^{-3}}}\right)^{-1/2}. \tag{I.2}$$

The Jeans mass is the amount of mass within a sphere of diameter λ_J, and corresponds intuitively to the minimum mass a core needs to gather in order to trigger a

gravitational collapse:

$$M_{\rm J} = \frac{4\pi}{3}\rho\left(\frac{\lambda_{\rm J}}{2}\right)^3, \tag{I.3}$$

$$= 0.3\,{\rm M}_\odot\left(\frac{c_{\rm s}}{0.2\,{\rm km\,s^{-1}}}\right)^3\left(\frac{n}{1000\,{\rm cm^{-3}}}\right)^{-1/2}. \tag{I.4}$$

Note that this formalism completely ignores the material that surrounds the core while it collapses. In practice, the cloud exerts an external pressure on the core that needs to be taken into account when calculating the critical masses. This case of a clump of self-gravitating gas that is immersed in a medium of external pressure $P_{\rm ext}$ is called a Bonnor-Ebert sphere. It can be shown (McKee et al., 2007) that the sizescale for a critical Bonnor-Ebert sphere is similar to the Jeans' length, and the mass scale is:

$$M_{\rm BE} = 1.18\frac{c_{\rm s}}{G^{3/2}\rho^{1/2}}, \tag{I.5}$$

$$= 4.4\,{\rm M}_\odot\left(\frac{c_{\rm s}}{0.2\,{\rm km\,s^{-1}}}\right)^3\left(\frac{n}{1000\,{\rm cm^{-3}}}\right)^{-1/2}, \tag{I.6}$$

$$\sim 14M_{\rm J}. \tag{I.7}$$

The turbulent nature of the core can lead to local overdensities which can reach the Jean's or Bonnor-Ebert masses. The core can then fragment into multiple centers of collapse, each of which will lead to a star. Accretion from the turbulent surrounding core material happens throughout this phase. A simple, symmetric accretion model features an infalling envelope with density profile which follow power laws from $r_{\rm env}^{-1.5}$ to $r_{\rm env}^{-2}$, an important observable that can be useful to test these theories. Some models of slowly-rotating infalling clouds suggest more complex density profiles for the envelopes (e.g. Ulrich, 1976; Terebey et al., 1984) than simple power laws, but are observationally difficult to

constrain due to the small differences with traditional power-law envelopes and the small scales at which those differences occur (a few 100's of astronomical units (au)).

Through conservation of angular momentum, some infalling material flattens into a circumstellar disk, while bipolar outflows carve out a cavity in the envelope along the axis of rotation of the star.

The object now has three characteristic components: the star itself; the flattened disk; and a diffuse envelope with an open cavity, which constitutes a mass reservoir for future accretion onto the star. A cartoon of the protostar is shown in Fig. I.1.

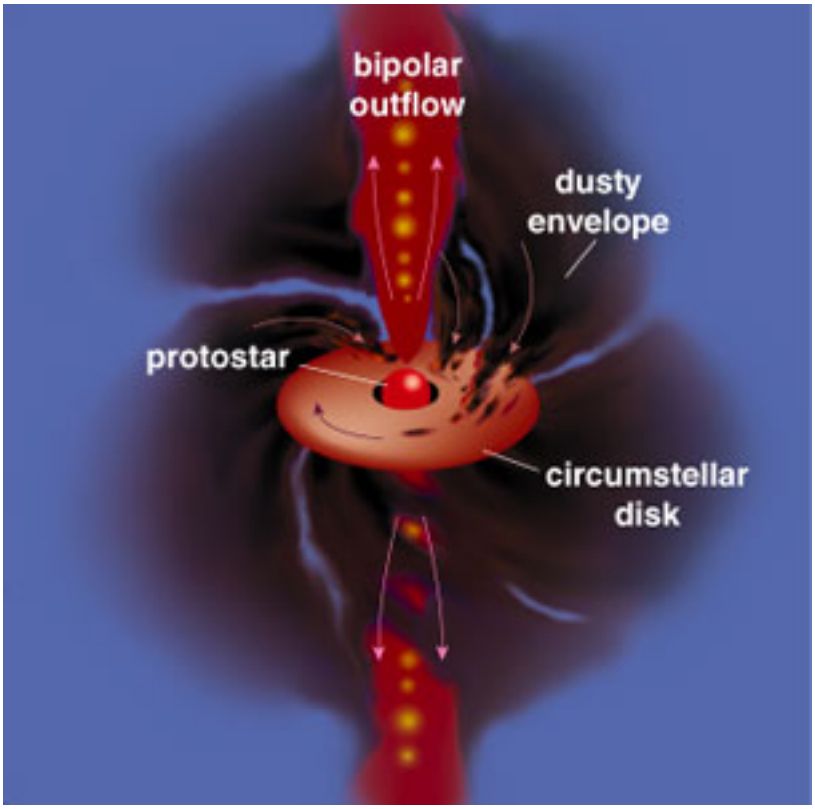

FIGURE I.1: Cartoon of a protostar (**Greene:2001dg**) with the envelope, a flattened circumstellar disk, the bipolar outflow/cavity, and the protostar at the center. A typical scale for the envelope of a young object is ∼10 000 au.

Although most of the mass is contained in the H_2 gas, there is a small fraction of material in the form of dust grains of various sizes and populations. Despite their low mass, these grains play a very important role in determining the observable properties of

YSOs, because of their tendency to absorb short wavelengths and radiate in the thermal infrared (see Section I.3).

I.2.1.2 YSO classification and characteristics

YSOs are composed of a star, a disk, and an envelope. The star is believed to be fairly well understood as a young object in hydrostatic equilibrium on its way to the main sequence. Depending on many parameters, the spatial distribution of gas in the disk and the envelope can be predicted by simple models, but in all likelihood is very complex, inhomogeneous, and asymmetric. For clarity, we will discuss here the simple models that can be used to describe the YSOs in the multiple stages of their evolution.

In the most common model of the evolution of young stars, there are four stages in the lifetime of a YSO. The first stage consists of a dense core right after the YSO is born. The disk is almost inexistent, the envelope still is dense and circularly symmetric. This is called Class 0. As the system evolves, the outflow increases the opening angle of the cavity, the density of the envelope decreases, and the size of the disk increases.

The various classes of YSO (from 0 to III) have distinct observational signatures, although can be dependent on the viewing angle. The most commonly used tool to classify YSOs based on their SEDs is to use the spectral index, which corresponds to the mid-IR slope α in the log-log plots, with $\alpha = \mathrm{d}(\log \lambda F_\lambda)/\mathrm{d}\log\lambda$ between 2 to 20 µm (McKee et al., 2007). The four classes of YSOs are:

- Class 0: Most the of short-wavelength (< 10 µm) light is highly obscured by the dust in the massive envelope. Most of the emission is around 100 µm and into the sub-millimeter/radio regimes. If there is a disk, it is very small. Some authors (Dunham

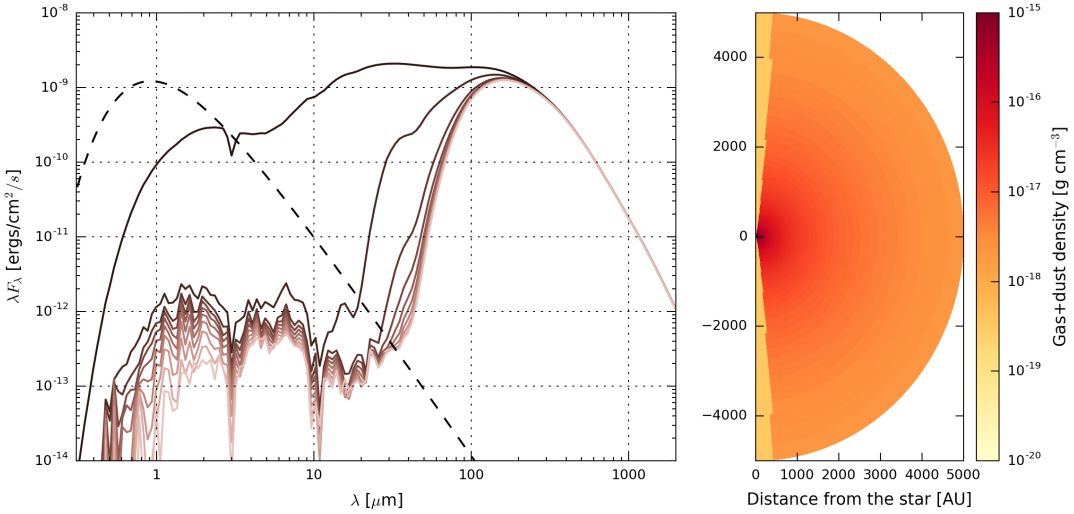

(a) Class 0

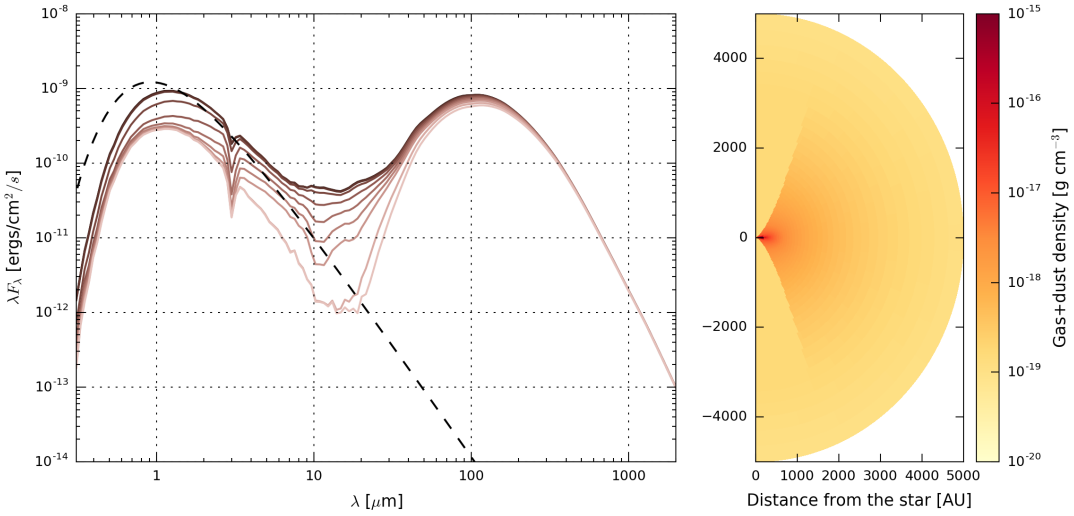

(b) Class I.

FIGURE I.2: Early evolution of YSOs. The left panel shows the spectral energy distribution (SED) of the object. Lines of different colors show different inclination angles. The dashed line corresponds to the SED of the central object only. The right panel shows a cross-section of the mass density (including both gas and dust) profile used in the modeling. Darker colors indicate higher densities. In this model, the cavity is in the up/down direction, coaligned with the circumstellar disk axis. The circumstellar disk is present in those models, although difficult to distinguish in the density maps because of its small scale.

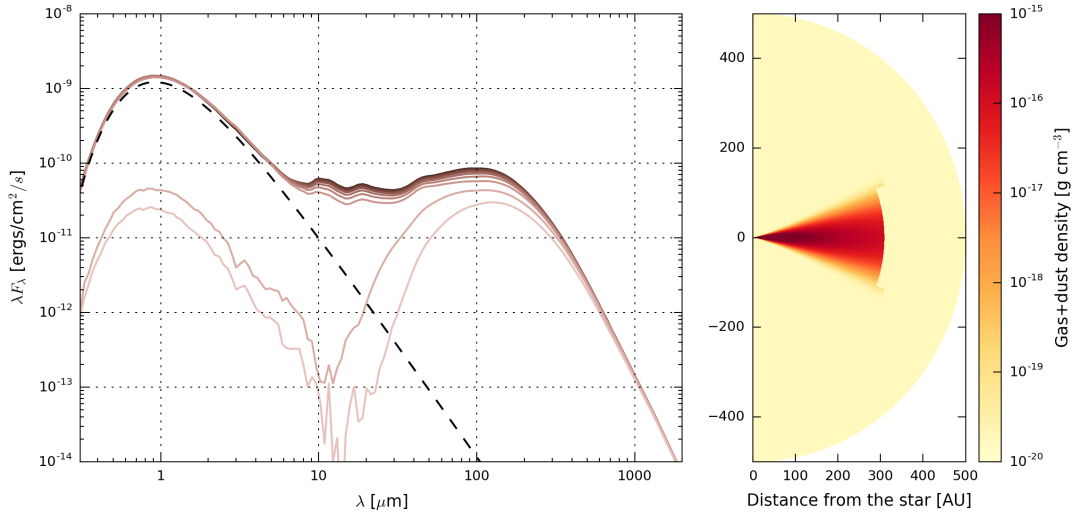

(a) Class II.

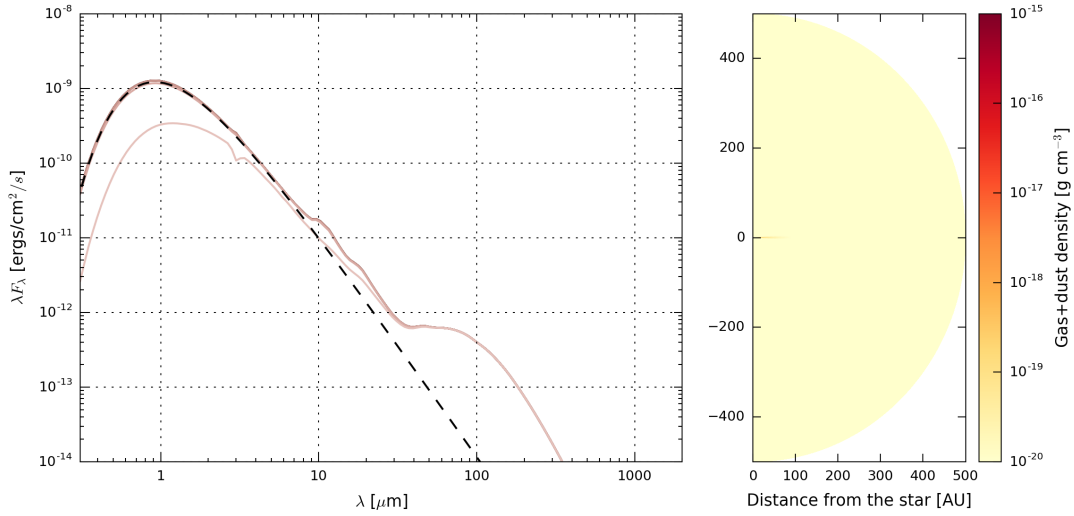

(b) Class III.

FIGURE I.3: Late evolution of YSOs.

et al., 2010) classify a source as Class 0 as long as the amount of the mass in the envelope is at least half the total mass.

- Class I: Light scatters at short wavelength off the dust grains to give us a hint at the embedded object, but it still very obscured. The envelope's mass is lower, and the disk extends to larger distances. The typical spectral index α is positive.

- Class II: The YSO is now a pre-main sequence star, with a spectral index $-1.5 < \alpha < 0$ and a significant circumstellar disk. This is traditionally referred to as a classical T-Tauri star.

- Class III: Still a pre-main sequence star, but most of the accretion has stopped, and $\alpha < -1.5$. The envelope has almost completely disappeared, and so has most or all of the disk, as traced by infrared excess emission.

An illustration of canonical spectral energy distributions (SED) and density structure is shown in Figs. I.2 and I.3 for the four main stages, with parameters taken in Whitney et al. (2003b). On the left of each picture, the SED is the measurable quantity when the YSO is unresolved at all wavelengths. The challenge is to estimate the density structure (to the right) by measuring the SED. The different lines plotted in the SEDs are different inclination angles, highlighting the enormous impact of the viewing angle on the potential interpretation of these SEDs. The dashed line corresponds to the Planck function from the central source. These models were run using the Hyperion software (Robitaille, 2011) with "OH5" dust (Ossenkopf et al., 1994), as discussed in more details in Section I.3.

These SEDs are often characterized and classified with standard observational metrics, such as the bolometric temperature and luminosities (Myers et al., 1993; Dunham et al., 2010):

$$L_{\rm bol} = 4\pi d^2 \int_0^\infty S_\nu d\nu, \tag{I.8}$$

$$T_{\rm bol} = 1.25 \times 10^{-11} \frac{\int_0^\infty \nu S_\nu d\nu}{\int_0^\infty S_\nu d\nu} \text{ K}, \tag{I.9}$$

where S_ν is the flux density in $\mathrm{W\,m^{-2}\,Hz^{-1}}$. We will use these simple diagnostics later in our analysis of our SOFIA FORCAST data.

I.2.2 Mass accretion in clusters

The discussion in the previous section represents a simplified view of how a single core collapses and forms a star. While it is convenient to assume that the original core forms a fixed reservoir of gas that will determine the star's final mass, it is likely too simplistic, since YSOs are preferentially forming inside of clusters close to multiple other YSOs and sharing a dense, often turbulent environment (Porras et al., 2003; Allen et al., 2007; Gutermuth et al., 2009).

The answer to how stars acquire their final mass is a key issue in star formation. Does dense gas fragment into isolated centers of collapse? Do young stars competitively accrete material from a surrounding common reservoir? Do gravitational interactions between forming young objects play a significant role in setting the final stellar mass function? Better observational understanding of these clusters is necessary to address these questions and to discriminate between the different models, as noted by Bonnell et al. (2006), Offner et al. (2011) and Myers (2011).

Given the typical stellar separations in clusters with fully formed YSOs and the typical densities of gas in these cores, several 1000s of au (1 pc = 206 265 au) is the size scale

over which forming stars must draw material to become 0.5-10 $M_\odot$. Once the material is inside a few 100s of au, it is strongly bound to the forming stellar system (which may be one or more stars) and its fate is determined. To give an idea of the possibilities for accreting material, Fig. I.4 sketches three scenarios for how stars could capture mass in the cluster environment: (a) core collapse, (b) competitive accretion, and (c) collisional merging. In core collapse (CC) (Fig. I.4a, McKee et al., 2003; Myers, 2011), the cluster's gas fragments into cores which collapse individually to form single, binary, or small multiple star systems; the available mass is defined by the original fragment. In competitive accretion (CA) (Fig. I.4b, Bonnell et al., 1997), the initial core collapses but contains a small fraction of the star's final mass; additional mass is captured competitively with other forming stars from the surrounding dense core gas. In collisional merging (CM) (Fig. I.4c, Bonnell et al., 2002), the initial fragments interact gravitationally and form larger mass cores before and during the formation process.

Are all these processes observed at once in star forming clusters? What conditions favor one versus the other, and why? Are these processes observed at different stages in the cluster's history?

Recent studies by Offner et al. (2011) and Myers (2011) compared protostar luminosity distributions with predictions of models based on these ideas. Offner et al. (2011) suggest that both CC and CA could work if the star formation rate in the cluster increases with time; (Myers, 2011) finds that a CA-type model with additional Bondi accretion to produce massive stars works best. As highlighted at the end of the Offner et al. (2011) paper, larger cluster samples and better data on massive stars are needed to improve the observational constraints on models.

(a) (b) (c)

FIGURE I.4: Three scenarios of clustered star formation: (a) core collapse, (b) competitive accretion, and (c) collisional merging. Darker colors indicate higher densities.

I.3 Dust as a tracer of star formation

Despite being a small component by mass, interstellar dust is an important tracer of star formation activity and its absorption and emission of radiation is an important factor in the evolution and outcome of the star formation process. Dust grains are heated up by absorbing the short wavelength emission from stars and re-radiate in the thermal infrared, accounting for $\sim 30\%$ of the total luminosity of the galaxy (Mathis, 1990).

Observationally, dust plays perhaps the most important role when it comes to studying star formation. It usually is assumed that dust is well mixed with the gas, which makes it an excellent tracer of the gravitational well and mass distribution in YSOs. Because H_2 and He molecules have very few spectral signatures at temperatures below 100 K, they are difficult to observe and study directly. Dust grains block UV and visible star light and emit continuum far-IR radiation, opening a large region of the electromagnetic spectrum for astronomers to study the properties of star formation. Alternative tools to study star formation are dedicated to observing spectral lines of the molecular species of the ISM such as CO and other dense gas tracers, which reveal information about the dynamics of

the gas in these regions.

I.3.1 Dust populations and properties

One of the best early studies of the composition of dust grains in the ISM was done by Mathis et al. (1977), where they studied the absorption spectrum of the diffuse ISM, and found that the measurements were appropriately fitted with a dust grain composition of silicates and small graphite particles (Stecher et al., 1965). They were able to fit the observed extinction curve with grain-size distribution, typically $n(a) \propto a^{-3.5}$, where a is the grain size (assuming spherical grains) and $n(a)$ corresponds to the number of grains of size a. This distributions requires low and high cutoffs for the grain sizes, typically 50 Å and 0.25 µm, respectively (Weingartner et al., 2001).

This grain size distribution model was later on enhanced by Cardelli et al. (1989) to account for the difference in interstellar extinctions (hence grain size distributions) across different galactic lines of sight. These authors were able to successfully parameterize the size distribution using a single parameter, R_V, which is the ratio of the total extinction $A(V)$ to selective extinction[1] (or color) $E(B-V) = A(B) - A(V)$. Smooth distributions of sizes of graphite and silicate grains vary between the low density regions of the ISM, where $R_V = 3.1$, and the high density regions, where $R_V = 5.3$ (Kim et al., 1994).

Observations in the thermal infrared from space telescopes have detected strong absorption lines at 9.7 µm and 18 µm which are attributed to stretching mode of Si-O and bending mode of O-Si-O, confirming the presence of silicates in dust compositions (Weingartner et al., 2001). Other emission features at 3.3, 6.2, 7.7, 8.6, and 11.3 µm (Sellgren, 1994) were attributed to bending and stretching modes of polycyclic aromatic

[1] Extinction and colors are expressed in magnitudes

hydrocarbons (PAH, see Gillett et al., 1973; Allamandola et al., 1985), which are complex, planar organic molecules.

A consolidated model matching all-sky measurements by COBE, IRAS and *Planck* confirms the composition of amorphous silicates and carbonaceous grains with sizes ranging from large grains ($\approx 1\,\mu m$) down to tens of atoms (**Collaboration:2016kp**), where the larger carbonaceous grains have graphitic properties and the smaller population have PAH-like properties.

Knowing the dust composition and size distribution of grains is important to properly predict its observational behavior and relate it to the physical quantities of interest, since the goal of the exercise is to use dust as a tracer of star-forming mechanisms. A given dust model needs to provide several key quantities that can be used in radiative transfer modeling (see Section I.3.3), such as the albedo, the scattering function, and the opacity.

In the very cold regions surrounding a YSO, where the dust temperature typically never exceeds a few tens of K, it is expected that these dust grains are covered by a mantel of ices which can dramatically change their radiative properties, especially at short wavelengths (e.g Ossenkopf et al., 1994).

I.3.2 Basics of dust extinction

Dust grains are responsible for the extinction within molecular clouds, inside of clusters, and also within each YSO; although these various extinctions could originate in different grain populations. The typical representation of this extinction uses the ratio of observed over expected flux, measured in V-band: $A_V \equiv A(V) = 2.5 \log(F_\nu^{\rm obs}/F_\nu)$. The extinction, $A(\lambda)$, is a function of wavelength and is expressed in magnitudes. An alternative representation is to consider the extinction as being caused by an optical depth $\tau_{\rm ext}$ such that

$\exp(-\tau_{\rm ext}) \equiv F_\nu^{\rm obs}/F_\nu$. The two definitions have the equivalence $A(\lambda) = 1.086\tau_{\rm ext}(\lambda)$.

At sufficiently long wavelength, dust opacity models can usually be represented by a simple power-law, $\kappa_\nu = \kappa_0(\nu/\nu_0)^\beta$, with the index β depending on the specifics of the dust model (**Draine:2011tr**). The opacity κ_ν is expressed in $\rm cm^2\,g^{-1}$, and can be interpreted as a extinction cross-section per unit mass. Most dust models assume a 1:100 dust-to-gas ratio, and derive opacities per unit gas+dust mass, instead of just dust mass. From a radiative transfer perspective, the observed specific intensity from a thermal source $B_\nu(T)$ at temperature T in the optically thin regime is $I_\nu = \int B_\nu(T) d\tau_\nu$, where the optical depth is $\tau_\nu = \int \kappa_\nu \rho_{\rm dust} dl$. In this expression all quantities depend on the location l along the line of sight. If T, $\kappa_n u$, and $\rho_{\rm dust}$ are constant along the line of sight, this simplifies to:

$$I_\nu = \tau_\nu B_\nu(T) = \kappa_n u \rho_{\rm dust} L B_\nu(T) = \kappa_n u \sigma_{\rm dust} B_\nu(T), \tag{I.10}$$

where we define $\sigma_{\rm dust}$ as the mass surface density.

A measure of the intensity from a source can thus lead to an approximation of the total mass within a primary beam, for a given dust grain model. For a source with a measured sub-millimeter flux density S_ν, in the optically thin regime we can write $S_\nu = \kappa_\nu \sigma_{\rm dust} B_\nu(T)\Omega$, where Ω is the solid angle of the source. We obtain a measure of the mass by writing $M \approx \sigma_{\rm dust}\Omega$, to obtain (e.g Shirley et al., 2000):

$$M = \frac{S_\nu d^2}{B_\nu(T_{\rm dust})\kappa_\nu}, \tag{I.11}$$

with a dust temperature is usually taken to be between 10 to 20 K for general regions of molecular clouds.

With only near- to mid-IR wavelengths observations (2-60 µm), however, it is more

difficult to estimate the dust mass, because the system is usually not in the optically thin regime and cool dust at these temperatures emits weakly or not at all at these wavelengths. To use these observations, which are interesting because they naturally are at higher resolution than single-dish submillimeter data, detailed radiative transfer models are usually required (see Section I.3.3).

Dust grains can either scatter or absorb photons, and both of these processes have their own frequency-dependent efficiency. Large grains are usually considered in local thermal equilibrium (LTE). However, small grains ($< 50\,\text{Å}$) can be subject to stochastic heating, where single photons can heat up the grains to much higher temperatures for very short amounts of time, which can cause the apparent temperature of the dust to be higher. In all cases the emission is expected to, and assumed, to be isotropic.

Scattering mechanisms can be much more complicated to represent, as they usually involve a scattering phase function, describing the deflection angle of incident photons (which also depends on wavelength). Most models show that dust grains are preferentially forward-scattering (**Draine:2011tr**). The scattering properties of the dust model strongly influence the short-wavelength flux, while the absorption properties influence all wavelengths.

I.3.3 Radiative transfer modeling

Several radiative transfer codes exist in the literature, and we have explored a few of them (DIRT, by **Wolfire:1986fw** HOCHUNK by Whitney et al. (2003a) and HOCHUNK3d by Whitney et al. (2013)). We opted for an open-source package called Hyperion (Robitaille, 2011), which has the advantage of having a Python interface and enjoys a relatively large community support. The code can accept different dust models and can generate various

types of geometries and density grids. It contains the essential geometrical elements of a YSO: stars, disks, envelopes with cavities, which all have numerous parameters to describe their density structures. It can also accept user-generated, arbitrary density grids.

Hyperion functions in two steps. The first is an iterative process that aims at determining the specific energy absorption rate of the dust in the grid. This is achieved for each dust population and each grid cell in the model. This can be linked to the temperature structure for each dust population, using pre-computed mean opacities and emissivities, as thoroughly explained in (Robitaille, 2011). Determining the specific energy absorption rate of the dust involves a Monte-Carlo technique that propagates photon packets across the grid and interacts with the dust in each cell. After choosing a discrete grid to represent a density model and adding energy sources, the temperature structure of the dust is calculated by propagating photon packets and determining the dust LTE temperature in each cell. Multiple iterations of this process are usually required to converge to a decent thermal structure.

Once the dust temperature is known, the dust becomes a source of thermal radiation. This type of radiation is modeled using ray tracing, which provides a very good signal-to-noise ratio (SNR). The light from the central source which was not absorbed, however, needs to be propagated and scattered off the dust grains, for example using a method called peeling-off (Yusef-Zadeh et al., 1984). For non-isotropic scattering, this process has relatively low SNR, hence requires a lot of photons packets to function properly. While there are future plans to implement raytracing for scattering (Robitaille, 2011), we are currently forced to wait long times for simulating YSOs with massive envelopes because of this problem.

[Put models of YSOs with different masses here?]

These models usually present a large amount of degeneracies, especially when the entire range of wavelengths is not covered, as it is the case for most astronomical sources. For example, an SED will look very different depending on the viewing angle. If we see down the throat of the cavity, the short-wavelength light from the central source will not exhibit a lot of extinction. If we observe this same source through the disk and envelope, these same wavelengths will show a lot of extinction since the light has to go through a large dust column.

Others (e.g., Robitaille et al., 2006) have used similar codes to produce standardized grids of pre-computed models which randomly sample a very large number of source geometry parameters. These grids of models are routinely used by the community to fit a set of unresolved SED measurements at discrete wavelengths. However, most often the scatter in the parameters for the few best fit models prevents from drawing meaningful conclusions on the observations. In Chapter **??**, we discuss this problem and offer an alternative method to determine the best-fitting models.

One of the key challenges of using this code is to determine which dust models to use. For this work, we choose to use exclusively OH5 dust (Ossenkopf et al., 1994), which represents grains with an ice mantle which are the result of a coagulation phase of an initial distribution of grain sizes following $n \propto a^{-3/2}$. This model was found to accurately represent some grain distribution in the ISM [NEED CITATION, CHECK OUT TRACY'S PAPER].

I.3.4 Observing star formation

In the past decade, space-based infrared observatories such as *Spitzer* and *Herschel* have really allowed the beginning of the detailed study of dust around forming stars, by sampling

the SEDs in key spectral regions, such as the PAH region (with the IRAC instrument on *Spitzer*), the mid-infrared (with the MIPS instrument, especially its 24 µm channel), and the far-IR (with the PACS and SPIRE instruments on *Herschel*). These single-aperture observatories have been excellent at changing our understanding of star formation on its largest scale.

However, these observatories lack the required angular resolution to observe the key physics of star formation in dense clusters in the key wavelength region between 30 µm and 200 µm. For a diffraction-limited single aperture telescope, the angular resolution and spatial resolutions R_θ and $R_{\rm linear}$ are:

$$R_\theta = 17.6'' \left(\frac{\lambda}{70\,\mu{\rm m}}\right)\left(\frac{D}{1\,{\rm m}}\right)^{-1}, \tag{I.12}$$

$$R_{\rm linear} = 0.04\,{\rm pc}\left(\frac{d}{500\,{\rm pc}}\right)\left(\frac{\lambda}{70\,\mu{\rm m}}\right)\left(\frac{D}{1\,{\rm m}}\right)^{-1}, \tag{I.13}$$

which shows that even *Herschel* with its 3.5 m primary mirror and its 70 µm channel can barely resolve clustered YSOs (typical separations of a few hundredths of pc) for the closest star-forming clusters, let alone study their structure in detail.

To further complicate the problem, most space observatories are tailored for very sensitive observations, so the brightest regions of clusters often cause saturation issues due to a lack of dynamic range to observe both the diffuse emission and the very clustered YSOs. These two issues have continually prevented scientists from gathering a good picture of the physics in these dense and important regions of stellar birth.

In the following chapter, we use SOFIA FORCAST to overcome both the lack of resolution of existing facilities, and the saturation effects from most observations towards

the densest regions of of star-forming regions. This is a first step towards a better understanding of these regions. This chapter is aimed at becoming a standalone publication in an astronomical journal, to be submitted shortly after the end of this thesis work.

Bibliography

Allamandola, L J, A G G M Tielens, and J R Barker (1985). "Polycyclic aromatic hydrocarbons and the unidentified infrared emission bands - Auto exhaust along the Milky Way". In: *Astrophysical Journal* 290, pp. L25–L28.

Allen, Christine A et al. (2006). "Far infrared through millimeter backshort-under-grid arrays". In: *Millimeter and Submillimeter Detectors and Instrumentation for Astronomy III. Edited by Zmuidzinas* 6275, 62750B–62750B–8.

Allen, L et al. (2007). "The Structure and Evolution of Young Stellar Clusters". In: *Protostars and Planets V*, p. 361.

Anglada, Guillem et al. (1998). "On the Exciting Sources of the L723 and IRAS 20050+2720 Quadrupolar Molecular Outflows". In: *Star Formation with the Infrared Space Observatory* 132, p. 303.

Astropy Collaboration et al. (2013). "Astropy: A community Python package for astronomy". In: A&A 558, A33, A33. DOI: 10.1051/0004-6361/201322068. arXiv: 1307.6212 [astro-ph.IM].

Bachiller, R, A Fuente, and M Tafalla (1995). "An extremely high velocity multipolar outflow around IRAS 20050 + 2720". In: *Astrophysical Journal* 445, pp. L51–L54.

Bachiller, Rafael (1996). "Bipolar Molecular Outflows from Young Stars and Protostars". In: *Annual Review of Astronomy and Astrophysics* 34.1, pp. 111–154.

Bally, J. (1982). "Energetic activity in a star-forming molecular cloud core - A disk constrained bipolar outflow in NGC 2071". In: ApJ 261, pp. 558–568. DOI: 10.1086/160366.

Beltrán, M T et al. (2008). "On the nature of outflows in intermediate-mass protostars: a case study of IRAS 20050+2720". In: *Astronomy and Astrophysics* 481.1, pp. 93–105.

Benford, Dominic J (2008). "Transition Edge Sensor Bolometers for CMB Polarimetry". In: *Workshop on Technology Development for a CMB Probe of Inflation*.

Bevington, Philip Raymond and D Keith Robinson (2003). *Data Reduction and Error Analysis for the Physical Sciences*. McGraw-Hill.

Blind, N et al. (2011). "Optimized fringe sensors for the VLTI next generation instruments". In: *Astronomy and Astrophysics* 530, p. 121.

Bonnell, I A et al. (1997). "Accretion and the stellar mass spectrum in small clusters". In: *Monthly Notices of the Royal Astronomical Society* 285, p. 201.

Bonnell, Ian A and Matthew R Bate (2002). "Accretion in stellar clusters and the collisional formation of massive stars". In: *Monthly Notice of the Royal Astronomical Society* 336.2, pp. 659–669.

— (2006). "Star formation through gravitational collapse and competitive accretion". In: *Monthly Notices of the Royal Astronomical Society* 370.1, pp. 488–494.

Bracco, A et al. (2011). "Herschel-ATLAS: statistical properties of Galactic cirrus in the GAMA-9 Hour Science Demonstration Phase Field". In: *Monthly Notices of the Royal Astronomical Society* 412.2, pp. 1151–1161.

Buckle, J. V. et al. (2010). "The JCMT Legacy Survey of the Gould Belt: a first look at Orion B with HARP". In: MNRAS 401, pp. 204–222. DOI: 10.1111/j.1365-2966.2009.15619.x. arXiv: 0908.4162.

Butner, H. M. et al. (1990). "High-resolution, far-infrared observations of NGC 2071". In: ApJ 364, pp. 164–172. DOI: 10.1086/169398.

Cardelli, Jason A, Geoffrey C Clayton, and John S Mathis (1989). "The relationship between infrared, optical, and ultraviolet extinction". In: *Astrophysical Journal* 345, pp. 245–256.

Carrasco-González, C. et al. (2012). "Multiplicity, Disks, and Jets in the NGC 2071 Star-forming Region". In: ApJ 746, 71, p. 71. DOI: 10.1088/0004-637X/746/1/71. arXiv: 1111.5469.

Chen, H et al. (1997). "IRAS 20050+2720: An Embedded Young Cluster Associated with a Multipolar Outflow". In: *The Astrophysical Journal* 475.1, pp. 163–172.

Chernin, L. and C. Masson (1993). "Observations of SO and SiO in the outflow from NGC 2071". In: ApJ 403, pp. L21–L24. DOI: 10.1086/186712.

Chini, R et al. (2001). "Mm/Submm images of Herbig-Haro energy sources and candidate protostars". In: *Astronomy and Astrophysics* 369.1, pp. 155–169.

Clauset, Aaron, Cosma Rohilla Shalizi, and M E J Newman (2007). "Power-law distributions in empirical data". In: *arXiv.org* 4, pp. 661–703. arXiv: 0706.1062v2 [physics.data-an].

Crassidis, John L and John L Junkins (2011). *Optimal Estimation of Dynamic Systems, Second Edition*. CRC Press.

Davis, Sumner P, Mark C Abrams, and James W Brault (2001). "Fourier transform spectrometry". In: *Fourier transform spectrometry by Sumner P. Davis et al. San Diego*.

De Buizer, James M et al. (2012). "First Science Observations with SOFIA/FORCAST: 6-37 μm Imaging of Orion BN/KL". In: *The Astrophysical Journal Letters* 749.2, p. L23.

Di Francesco, J et al. (2007). "An Observational Perspective of Low-Mass Dense Cores I: Internal Physical and Chemical Properties". In: *Protostars and Planets V*, pp. 17–32.

Dishoeck, E F van et al. (2011). "Water in Star-forming Regions with the Herschel Space Observatory (WISH). I. Overview of Key Program and First Results". In: *Publications of the Astronomical Society of Pacific* 123.9, pp. 138–170.

Dunham, Michael M et al. (2010). "Evolutionary Signatures in the Formation of Low-Mass Protostars. II. Toward Reconciling Models and Observations". In: *The Astrophysical Journal* 710.1, pp. 470–502.

El Badaoui, Noad et al. (2014). "Towards a solid-state ring laser gyroscope". In: *Comptes Rendus Physique* 15.10, pp. 841–850.

Elias, Nicholas M et al. (2007). "The Mathematics of Double-Fourier Interferometers". In: *The Astrophysical Journal* 657.2, pp. 1178–1200.

Enoch, Melissa L et al. (2009). "Properties of the Youngest Protostars in Perseus, Serpens, and Ophiuchus". In: *The Astrophysical Journal* 692.2, pp. 973–997.

Evans II, N. J. et al. (2009). "The Spitzer c2d Legacy Results: Star-Formation Rates and Efficiencies; Evolution and Lifetimes". In: ApJS 181, 321, pp. 321–350. DOI: 10.1088/0067-0049/181/2/321. arXiv: 0811.1059.

Evans, Neal J et al. (2009). "The Spitzer c2d Legacy Results: Star-Formation Rates and Efficiencies; Evolution and Lifetimes". In: *The Astrophysical Journal Supplement* 181.2, pp. 321–350.

Ferrière, Katia M (2001). "The interstellar environment of our galaxy". In: *Reviews of Modern Physics* 73.4, pp. 1031–1066.

Fischer, William J et al. (2012). "Multiwavelength Observations of V2775 Ori, an Outbursting Protostar in L 1641: Exploring the Edge of the FU Orionis Regime". In: *The Astrophysical Journal* 756.1, p. 99.

Fixsen, D J and Eli Dwek (2002). "The Zodiacal Emission Spectrum as Determined by COBE and Its Implications". In: *The Astrophysical Journal* 578.2, pp. 1009–1014.

Fixsen, D J and J C Mather (2002). "The Spectral Results of the Far-Infrared Absolute Spectrophotometer Instrument on COBE". In: *The Astrophysical Journal* 581.2, pp. 817–822.

Fixsen, D J et al. (1996a). "A Balloon-borne Millimeter-Wave Telescope for Cosmic Microwave Background Anisotropy Measurements". In: *Astrophysical Journal v.470* 470, p. 63.

Fixsen, D J et al. (1996b). "The Cosmic Microwave Background Spectrum from the Full COBE FIRAS Data Set". In: *Astrophysical Journal v.473* 473.2, pp. 576–587.

Fixsen, D J et al. (1998). "The Spectrum of the Extragalactic Far-Infrared Background from the COBE FIRAS Observations". In: *The Astrophysical Journal* 508.1, pp. 123–128.

Flaherty, K. M. and J. Muzerolle (2008). "Evidence for Early Circumstellar Disk Evolution in NGC 2068/71". In: AJ 135, pp. 966–983. DOI: 10.1088/0004-6256/135/3/966. arXiv: 0712.1601.

Fontani, F, R Cesaroni, and R S Furuya (2010). "Class I and Class II methanol masers in high-mass star-forming regions". In: *Astronomy and Astrophysics* 517, A56.

Forman, Michael L, W Howard Steel, and George A Vanasse (1966). "Correction of Asymmetric Interferograms Obtained in Fourier Spectroscopy". In: *Journal of the Optical Society of America* 56, p. 59.

Furlan, E et al. (2016). "The Herschel Orion Protostar Survey: Spectral Energy Distributions and Fits Using a Grid of Protostellar Models". In: *The Astrophysical Journal Supplement Series* 224.1, p. 5.

Gillett, F C, W J Forrest, and K M Merrill (1973). "8 - 13-micron spectra of NGC 7027, BD +30 3639, and NGC 6572." In: *Astrophysical Journal* 183, pp. 87–93.

Grainger, William F et al. (2012). "Demonstration of spectral and spatial interferometry at THz frequencies". In: *Applied Optics* 51.12, pp. 2202–2211.

Griffiths, Peter R and James A De Haseth (2007). *Fourier Transform Infrared Spectrometry.* John Wiley & Sons.

Günther, H M et al. (2012). "IRAS 20050+2720: Anatomy of a Young Stellar Cluster". In: *The Astronomical Journal* 144.4, p. 101.

Gutermuth, R A et al. (2009). "A Spitzer Survey of Young Stellar Clusters Within One Kiloparsec of the Sun: Cluster Core Extraction and Basic Structural Analysis". In: *The Astrophysical Journal Supplement* 184.1, pp. 18–83.

Gutermuth, R A et al. (2011). "A Correlation between Surface Densities of Young Stellar Objects and Gas in Eight Nearby Molecular Clouds". In: *The Astrophysical Journal* 739.2, p. 84.

Gutermuth, Robert A et al. (2005). "The Initial Configuration of Young Stellar Clusters: A K-Band Number Counts Analysis of the Surface Density of Stars". In: *The Astrophysical Journal* 632.1, pp. 397–420.

Harman, Richard R (2005). *Wilkinson Microwave Anisotropy Probe (WMAP) Attitude Estimation Filter Comparison.*

Harries, J E (1980). "Atmospheric radiometry at submillimeter wavelengths". In: *Applied Optics* 19.18, p. 3075.

Harvey, P. M. et al. (1979). "Infrared observations of NGC 2071/IRS/ and AFGL 490 - Two low-luminosity young stars". In: ApJ 229, pp. 990–993. DOI: 10.1086/157033.

Harvey, Paul M et al. (2012). "First Science Results from SOFIA/FORCAST: Super-resolution Imaging of the S140 Cluster at 37 μm". In: *The Astrophysical Journal Letters* 749.2, p. L20.

Harwit, Martin, David Leisawitz, and Stephen Rinehart (2006). "A far-infrared/submillimeter kilometer-baseline interferometer in space". In: *New Astronomy Reviews* 50.1-3, pp. 228–234.

Helmich, Frank P and R J Ivison (2009). "FIRI—A far-infrared interferometer". In: *Experimental Astronomy* 23.1, pp. 245–276.

Herter, T L et al. (2012). "First Science Observations with SOFIA/FORCAST: The FORCAST Mid-infrared Camera". In: *The Astrophysical Journal Letters* 749.2, p. L18.

Herter, T L et al. (2013). "Data Reduction and Early Science Calibration for FORCAST, A Mid-Infrared Camera for SOFIA". In: *Publications of the Astronomical Society of the Pacific* 125.933, pp. 1393–1404.

Johnstone, D. et al. (2001). "Large Area Mapping at 850 Microns. III. Analysis of the Clump Distribution in the Orion B Molecular Cloud". In: ApJ 559, pp. 307–317. DOI: 10.1086/322323.

Kalman, R E (1960). "A New Approach to Linear Filtering and Prediction Problems". In: *Journal of Basic Engineering* 82.1, pp. 35–45.

Kato, Eri et al. (2010). "Far-Infrared Interferometric Telescope Experiment : I. Interferometer Optics". In: *Transactions of Space Technology Japan* 7.ists26, pp. 47–53.

Kempen, T A van et al. (2009). "The nature of the Class I population in Ophiuchus as revealed through gas and dust mapping". In: *Astronomy and Astrophysics* 498.1, pp. 167–194.

Kempen, T A van et al. (2012). "The Small-scale Physical Structure and Fragmentation Difference of Two Embedded Intermediate-mass Protostars in Orion". In: *The Astrophysical Journal* 751.2, p. 137.

Kennicutt, R. C. and N. J. Evans (2012). "Star Formation in the Milky Way and Nearby Galaxies". In: ARA&A 50, pp. 531–608. DOI: 10.1146/annurev-astro-081811-125610. arXiv: 1204.3552.

Kennicutt, Robert C and Neal J Evans (2012). "Star Formation in the Milky Way and Nearby Galaxies". In: *Annual Review of Astronomy and Astrophysics* 50.1, pp. 531–608.

Kessler, M F et al. (1996). "The Infrared Space Observatory (ISO) mission." In: *Astronomy and Astrophysics* 315, pp. L27–L31.

Kim, Sang-Hee, P G Martin, and Paul D Hendry (1994). "The size distribution of interstellar dust particles as determined from extinction". In: *Astrophysical Journal* 422, pp. 164–175.

Korte, Piet A J de et al. (2003). "Time-division superconducting quantum interference device multiplexer for transition-edge sensors". In: *Review of Scientific Instruments* 687.8, pp. 3807–3815.

Lada, Charles J and Elizabeth A Lada (2003). "Embedded Clusters in Molecular Clouds". In: *Annual Review of Astronomy &Astrophysics* 41.1, pp. 57–115.

Lada, E. A. et al. (1991). "A 2.2 micron survey in the L1630 molecular cloud". In: ApJ 371, pp. 171–182. DOI: 10.1086/169881.

Larson, R B (1994). "The Evolution of Molecular Clouds". In: *The Structure and Content of Molecular Clouds* 439.Chapter 2, pp. 13–28.

Launhardt, R. et al. (1996). "Dust emission from star-forming regions. IV. Dense cores in the Orion B molecular cloud." In: A&A 312, pp. 569–584.

Lawson, Peter R (2000). "Principles of Long Baseline Stellar Interferometry". In: *Principles of Long Baseline Stellar Interferometry. Course notes from the 1999 Michelson Summer School*.

Lefferts, E J, F L Markley, and M D Shuster (1982). "Kalman Filtering for Spacecraft Attitude Estimation". In: *Journal of Guidance* 5.5, pp. 417–429.

Leisawitz, David et al. (2007). "The space infrared interferometric telescope (SPIRIT): High-resolution imaging and spectroscopy in the far-infrared". In: *Advances in Space Research* 40.5, pp. 689–703.

Leisawitz, David et al. (2012). "Developing wide-field spatio-spectral interferometry for far-infrared space applications". In: *Optical and Infrared Interferometry III. Proceedings of the SPIE*. Ed. by Françoise Delplancke, Jayadev K Rajagopal, and Fabien Malbet. NASA Goddard Space Flight Ctr. (United States). SPIE, 84450A.

Li, Aigen and B T Draine (2001). "Infrared Emission from Interstellar Dust. II. The Diffuse Interstellar Medium". In: *The Astrophysical Journal* 554.2, pp. 778–802.

Mariotti, J-M and S T Ridgway (1988). "Double Fourier spatio-spectral interferometry - Combining high spectral and high spatial resolution in the near infrared". In: *Astronomy and Astrophysics (ISSN 0004-6361)* 195, p. 350.

Markley, F Landis and John L Crassidis (2014). *Fundamentals of Spacecraft Attitude Determination and Control*. New York, NY: Springer.

Mathis, J S, W Rumpl, and K H Nordsieck (1977). "The size distribution of interstellar grains". In: *Astrophysical Journal* 217, pp. 425–433.

Mathis, John S (1990). "Interstellar dust and extinction". In: *IN: Annual review of astronomy and astrophysics. Vol. 28 (A91-28201 10-90). Palo Alto* 28.1, pp. 37–70.

Matsumoto, T, S Matsuura, and M Noda (1994). "2.4 micrometer sky brightness at balloon altitude". In: *Astronomical Society of the Pacific* 106, p. 1217.

Maybeck, Peter S (1982). *Stochastic Models, Estimation, and Control*. Academic Press.

McKee, Christopher F and Eve C Ostriker (2007). "Theory of Star Formation". In: *Annual Review of Astronomy and Astrophysics* 45.1, pp. 565–687.

McKee, Christopher F and Jonathan C Tan (2003). "The Formation of Massive Stars from Turbulent Cores". In: *The Astrophysical Journal* 585.2, pp. 850–871.

Megeath, S T et al. (2012). "The Spitzer Space Telescope Survey of the Orion A and B Molecular Clouds. I. A Census of Dusty Young Stellar Objects and a Study of Their Mid-infrared Variability". In: *The Astronomical Journal* 144.6, p. 192.

Megeath, S. T. et al. (2012). "The Spitzer Space Telescope Survey of the Orion A and B Molecular Clouds. I. A Census of Dusty Young Stellar Objects and a Study of Their Mid-infrared Variability". In: AJ 144, 192, p. 192. DOI: 10.1088/0004-6256/144/6/192. arXiv: 1209.3826.

Mendillo, Christopher B et al. (2012). "Flight demonstration of a milliarcsecond pointing system for direct exoplanet imaging". In: *Applied Optics* 51.29, p. 7069.

Meynart, Roland (1992). "Sampling jitter in Fourier-transform spectrometers - Spectral broadening and noise effects". In: *Applied Optics (ISSN 0003-6935)* 31.30, p. 6383.

Michelson, Albert A and Edward W Morley (1887). "On the Relative Motion of the Earth and of the Luminiferous Ether". In: *Sidereal Messenger* 6, pp. 306–310.

Mighell, Kenneth J (2005). "Stellar photometry and astrometry with discrete point spread functions". In: *Monthly Notices of the Royal Astronomical Society* 361.3, pp. 861–878.

Mitchell, G. F. et al. (2001). "A Submillimeter Dust and Gas Study of the Orion B Molecular Cloud". In: ApJ 556, pp. 215–229. DOI: 10.1086/321574.

Molinari, S et al. (1996). "A search for precursors of ultracompact HII regions in a sample of luminous IRAS sources. I. Association with ammonia cores." In: *Astronomy and Astrophysics* 308, pp. 573–587.

Murakami, H et al. (2007). "The Infrared Astronomical Mission AKARI". In: *Publications of the Astronomical Society of Japan* 59.sp2, 369–S376.

Myers, P C and E F Ladd (1993). "Bolometric temperatures of young stellar objects". In: *Astrophysical Journal* 413, pp. L47–L50.

Myers, Philip C (2011). "Star Formation in Dense Clusters". In: *The Astrophysical Journal* 743.1, p. 98.

Neugebauer, G et al. (1984). "The Infrared Astronomical Satellite (IRAS) mission". In: *Astrophysical Journal* 278, pp. L1–L6.

Offner, Stella S R and Christopher F McKee (2011). "The Protostellar Luminosity Function". In: *The Astrophysical Journal* 736.1, p. 53.

Ossenkopf, V and Th Henning (1994). "Dust opacities for protostellar cores". In: *Astronomy and Astrophysics (ISSN 0004-6361)* 291, pp. 943–959.

Oxley, Paul et al. (2004). "The EBEX experiment". In: *Infrared Spaceborne Remote Sensing XII. Edited by Strojnik* 5543, pp. 320–331.

Palla, F et al. (1991). "Water masers associated with dense molecular clouds and ultracompact H II regions". In: *Astronomy and Astrophysics (ISSN 0004-6361)* 246, pp. 249–263.

Peltier, JCA (1834). *Investigation of the heat developed by electric currents in homogeneous materials and at the junction of two different conductors.* Ann. Chim. Phys.

Persson, S. E. et al. (1981). "High Velocity h2 Line Emission in the NGC2071 Region". In: ApJ 251, p. L85. DOI: 10.1086/183699.

Pilbratt, G L et al. (2010). "Herschel Space Observatory. An ESA facility for far-infrared and submillimetre astronomy". In: *Astronomy and Astrophysics* 518, p. L1.

Porras, Alicia et al. (2003). "A Catalog of Young Stellar Groups and Clusters within 1 Kiloparsec of the Sun". In: *The Astronomical Journal* 126.4, pp. 1916–1924.

Press, William H et al. (1992). "Numerical recipes in C. The art of scientific computing". In: *Cambridge: University Press.*

Richards, M A (2003). "Coherent integration loss due to white gaussian phase noise". In: *IEEE Signal Processing Letters* 10.7, pp. 208–210.

Rinehart, S A et al. (2014). "The Balloon Experimental Twin Telescope for Infrared Interferometry (BETTII): An Experiment for High Angular Resolution in the Far-Infrared". In: *Publications of the Astronomical Society of the Pacific* 126, pp. 660–673.

Rizzo, Maxime J et al. (2012). "Tracking near-infrared fringes on BETTII: a balloon-borne, 8m-baseline interferometer". In: *Optical and Infrared Interferometry III. Proceedings of the SPIE* 8445, 84451T.

Rizzo, Maxime J et al. (2014). "Building an interferometer at the edge of space: pointing and phase control system for BETTII". In: *Proceedings of the SPIE*. Ed. by Jacobus M Oschmann et al. Univ. of Maryland, College Park (United States). SPIE, 91433H–91433H–12.

Rizzo, Maxime J et al. (2015). "Far-Infrared Double-Fourier Interferometers and their Spectral Sensitivity". In: *Publications of the Astronomical Society of Pacific* 127.9, pp. 1045–1060.

Robitaille, T P (2011). "HYPERION: an open-source parallelized three-dimensional dust continuum radiative transfer code". In: *Astronomy and Astrophysics* 536, A79.

Robitaille, Thomas P et al. (2006). "Interpreting Spectral Energy Distributions from Young Stellar Objects. I. A Grid of 200,000 YSO Model SEDs". In: *The Astrophysical Journal Supplement Series* 167.2, pp. 256–285.

Robitaille, Thomas P et al. (2007). "Interpreting Spectral Energy Distributions from Young Stellar Objects. II. Fitting Observed SEDs Using a Large Grid of Precomputed Models". In: *The Astrophysical Journal Supplement Series* 169.2, pp. 328–352.

Sellgren, K (1994). "Tiny Grains, Large Molecules, and the Infrared Cirrus". In: *The First Symposium on the Infrared Cirrus and Diffuse Interstellar Clouds. ASP Conference Series* 58, pp. 243–.

Shimizu, T Taro et al. (2016). "Herschel far-infrared photometry of the Swift Burst Alert Telescope active galactic nuclei sample of the local universe - II. SPIRE observations". In: *Monthly Notices of the Royal Astronomical Society* 456.3, pp. 3335–3353.

Shirley, Yancy L et al. (2000). "Tracing the Mass during Low-Mass Star Formation. I. Submillimeter Continuum Observations". In: *The Astrophysical Journal Supplement Series* 131.1, pp. 249–271.

Shu, F H (1977). "Self-similar collapse of isothermal spheres and star formation". In: *Astrophysical Journal* 214, pp. 488–497.

Skinner, S. L. et al. (2009). "Chandra and Spitzer Imaging of the Infrared Cluster in NGC 2071". In: ApJ 701, pp. 710–724. DOI: 10.1088/0004-637X/701/1/710. arXiv: 0906.2428 [astro-ph.SR].

Spezzi, L. et al. (2015). "The VISTA Orion mini-survey: star formation in the Lynds 1630 North cloud". In: *ArXiv e-prints*. arXiv: 1505.04631 [astro-ph.SR].

Sromovsky, Lawrence A (2003). "Radiometric Errors in Complex Fourier Transform Spectrometry". In: *Applied Optics OT* 42.10, p. 1779.

Staguhn, Johannes et al. (2014a). "Design and Expected Performance of GISMO-2, a Two Color Millimeter Camera for the IRAM 30 m Telescope". In: *Journal of Low Temperature Physics* 176.5, pp. 829–834.

Staguhn, Johannes G et al. (2014b). "The GISMO Two-millimeter Deep Field in GOODS-N". In: *The Astrophysical Journal* 790.1, p. 77.

Stecher, T P and B Donn (1965). "On Graphite and Interstellar Extinction". In: *Astrophysical Journal* 142, pp. 1681–.

Stojimirović, I., R. L. Snell, and G. Narayanan (2008). "Multiple Parsec-Scale Outflows in the NGC 2071 Cluster". In: ApJ 679, pp. 557–569. DOI: 10.1086/586688.

Strom, K. M., S. E. Strom, and F. J. Vrba (1976). "Infrared surveys of dark-cloud complexes. I. The Lynds 1630 dark cloud." In: AJ 81, pp. 308–313. DOI: 10.1086/111888.

Tan, J C et al. (2014). "Massive Star Formation". In: *Protostars and Planets VI*, pp. 149–172.

Terebey, S, F H Shu, and P Cassen (1984). "The collapse of the cores of slowly rotating isothermal clouds". In: *Astrophysical Journal* 286, pp. 529–551.

Thompson, A Richard, James M Moran, and Jr George W Swenson (2008). *Interferometry and Synthesis in Radio Astronomy*. John Wiley & Sons.

Trawny, N and S I Roumeliotis (2005). "Indirect Kalman filter for 3D attitude estimation". In:

Ulrich, R K (1976). "An infall model for the T Tauri phenomenon". In: *Astrophysical Journal* 210, pp. 377–391.

van Kempen, T. A. et al. (2012). "The Small-scale Physical Structure and Fragmentation Difference of Two Embedded Intermediate-mass Protostars in Orion". In: ApJ 751, 137, p. 137. DOI: 10.1088/0004-637X/751/2/137. arXiv: 1203.3718.

Weingartner, Joseph C and B T Draine (2001). "Dust Grain-Size Distributions and Extinction in the Milky Way, Large Magellanic Cloud, and Small Magellanic Cloud". In: *The Astrophysical Journal* 548.1, pp. 296–309.

Werner, M W et al. (2004). "The Spitzer Space Telescope Mission". In: *The Astrophysical Journal Supplement Series* 154.1, pp. 1–9.

Whitney, B A et al. (2013). "Three-dimensional Radiation Transfer in Young Stellar Objects". In: *The Astrophysical Journal Supplement* 207.2, p. 30.

Whitney, Barbara A et al. (2003a). "2-D Radiative Transfer in Protostellar Envelopes: I. Effects of Geometry on Class I Sources". In: *arXiv.org* 2, pp. 1049–1063. arXiv: astro-ph/0303479v1 [astro-ph].

Whitney, Barbara A et al. (2003b). "Two-dimensional Radiative Transfer in Protostellar Envelopes. II. An Evolutionary Sequence". In: *The Astrophysical Journal* 598.2, pp. 1079–1099.

Wilking, B A et al. (1989). "A millimeter-wave spectral-line and continuum survey of cold IRAS sources". In: *Astrophysical Journal* 345, pp. 257–264.

Williams, J P, L Blitz, and C F McKee (2000). "The Structure and Evolution of Molecular Clouds: from Clumps to Cores to the IMF". In: *Protostars and Planets IV (Book - Tucson: University of Arizona Press; eds Mannings*, pp. 97–.

Wright, Edward L et al. (2010). "The Wide-field Infrared Survey Explorer (WISE): Mission Description and Initial On-orbit Performance". In: *The Astronomical Journal* 140.6, pp. 1868–1881.

Yusef-Zadeh, F, M Morris, and R L White (1984). "Bipolar reflection nebulae - Monte Carlo simulations". In: *Astrophysical Journal* 278, pp. 186–194.

Zernike, F (1938). "The concept of degree of coherence and its application to optical problems". In: *Physica* 5.8, pp. 785–795.

Zhou, S., N. J. Evans II, and L. G. Mundy (1990). "An NH3 ring around the infrared sources in NGC 2071". In: ApJ 355, pp. 159–165. DOI: 10.1086/168749.